FDTD Analysis of a Probe-Fed Dielectric Resonator Antenna in Rectangular Waveguide

Yizhe Zhang, Ahmed A. Kishk, Alexander B. Yakovlev*, and Allen W. Glisson
Department of Electrical Engineering
Center of Applied Electromagnetic Systems Research
The University of Mississippi, University, MS, 38677, USA
zyz@olemiss.edu, ahmed@olemiss.edu, yakovlev@olemiss.edu,
aglisson@olemiss.edu

Abstract: A probe-fed dielectric resonator antenna (DRA) element is investigated for operation in a waveguide environment with application to spatial power combining amplifier arrays. The method of analysis is based on the finite-difference time-domain (FDTD) approach, wherein a rectangular waveguide and DRA are discretized by using a traditional Yee cell griding and a coaxial line is modeled by a thin wire approximation. The input impedance and scattering parameters are studied by varying geometrical and material parameters of the DRA and the coaxial probe feed. The numerical results obtained by the proposed FDTD method are compared with those generated by using a commercial software and exhibit very good agreement.

Keywords: Dielectric resonator antenna, rectangular waveguide, finite-difference time-domain method

1. Introduction

In recent years, there has been an increasing demand for high-power and efficient solid-state microwave and millimeter-wave amplifiers, which resulted in extensive experimental and theoretical research in the area of quasi-optical and spatial power combining. A new generation of spatial/quasi-optical power combiners requires a development of integrated modeling environment in order to design systems with high output power levels and power combining efficiencies for operation at millimeter-wave frequencies. Thus, receive and transmit antenna elements used in the amplifier arrays must be carefully selected and accurately modeled.

Due to their attractive characteristics, DRA elements have received an increasing interest as radiating antenna elements. The DRA elements have many advantages such as wideband nature, small size, high power handling capability, and high radiation efficiency as compared with microstrip antennas [1]-[3]. The DRA is often made of high dielectric constant materials with very low loss tangent, which makes it attractive for high frequency applications where the conduction loss will be much smaller than that of microstrip antennas.

In this paper, a coaxial probe-fed DRA is studied for operation in a rectangular waveguide for potential application in spatial power combining amplifier arrays. The FDTD method is used for the full-wave analysis of the structure. Scattering parameters of the waveguide-based DRA are studied by varying a position and length of the excitation probe and by changing the geometrical parameters of the DRA.

In the next section, a brief description of the analysis method is presented. In Section 3, the scattering parameters are computed using the FDTD method and are compared with the results obtained using commercial software. Conclusions and discussions are presented in Section 4.

2. Theory

The structure to be analyzed here consists of a coaxial probe-fed DRA inside a rectangular waveguide as shown in Fig. 1. The geometry is modeled by using the FDTD method, where the PML absorbing boundary condition is used to terminate both the waveguide port and the coaxial line. For the waveguide calculation area, the traditional FDTD update equations are used. The inner conductor of the coaxial line is modeled by a thin wire approximation, when the radius is smaller than the FDTD cell dimensions [4]. With $E_z(i, j, k) = 0$ along the wire axis, the spatial dependence of the fields in the vicinity can be calculated by

$$H_y^{n+\frac{1}{2}}(i,j,k) = H_y^{n-\frac{1}{2}}(i,j,k) + \frac{\Delta t}{\mu \Delta z}\left[E_x^n(i,j,k) - E_x^n(i,j,k+1)\right] + \frac{2\Delta t}{\mu \Delta x \ln\left(\frac{\Delta x}{r_0}\right)} E_z^n(i+1,j,k). \quad (1)$$

The time domain incident and total modal voltages can be calculated from the total electric field as

$$V_S(z_0,t) = \iint \vec{E}(x,y,z_0,t)\cdot \vec{e}_S(x,y)\,dxdy \quad (2)$$

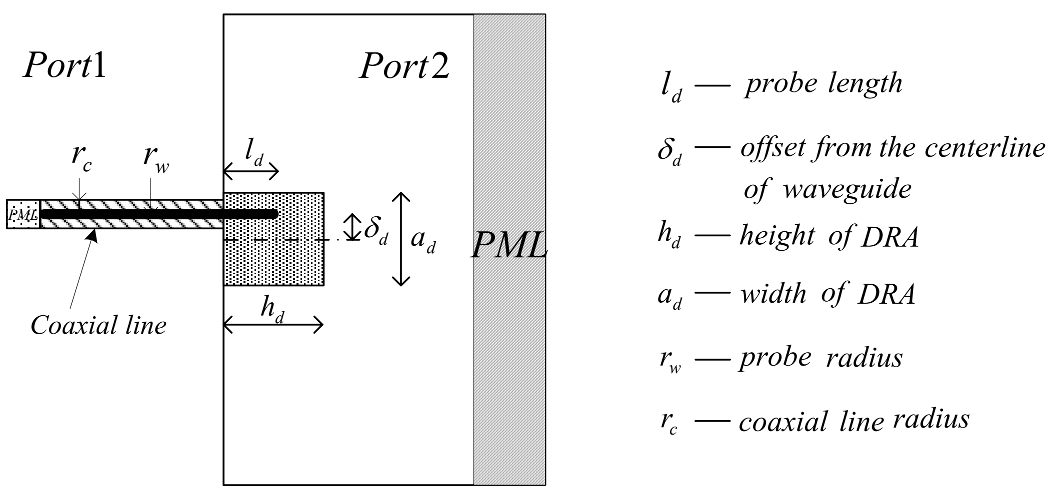

Fig. 1. Waveguide-based coaxial probe-fed DRA geometry.

where V_S is the time domain modal voltage for the mode S at the transverse plane located at $z = z_0$, $\vec{E}$ is the time domain total electric field in a rectangular waveguide due to the excitation across a waveguide transverse plane, $\vec{e}_S$ is the modal field vector [5] for the mode S, and the integral in (2) is over the transverse plane of the waveguide port.

The scattering parameters can be calculated as a ratio of port voltages normalized by the characteristic impedances, which for the waveguide section with a coaxial probe-fed DRA, are given by

$$S_{11} = \frac{V^-_{waveguide}}{V^+_{waveguide}} = \frac{V_{waveguide\_total} - V^+_{waveguide}}{V^+_{waveguide}} \ , \ S_{21} = \frac{V^+_{coaxial}}{V^+_{waveguide}} \sqrt{\frac{Z_{waveguide}}{Z_{coaxial}}} \tag{3}$$

where V^- is the voltage calculated from the reflection field, V^+ is the voltage calculated from the forward traveling wave, and the Z's are the characteristic impedances. The characteristic impedance of the coaxial line can be calculated in terms of currents and voltages as explained in [5].

3. Results and Discussion

The initial dimensions of the DRA structure are chosen so that the resonance frequency of the $TE_{11\delta}$ mode is centered around 10 GHz [6]. First, commercial method of moments (MoM) software [7] was used for the approximate analysis of a single probe-fed DRA element placed on an infinite ground plane and radiating in free space as shown in Fig. 2(a), where a_d= 5.0 mm, h_d = 12.0 mm, δ_d = 1.0 mm, ε_{rd} = 12, and the probe radius r_w is 0.3 mm. Then, the probe-fed DRA was placed into a semi-infinite standard X-band waveguide of cross-sectional dimensions a =22.86 mm and b =10.16 mm (with geometry shown in Fig. 2(b)). To take into consideration the effect of waveguide walls, the height of the DRA and the probe position were changed to h_d = 9.5 mm and δ_d = 1.5 mm, respectively. Figs. 3 and 4 show dispersion behavior of the input impedance and the reflection coefficient for the geometries shown in Fig. 2 (a) and (b) (cases (a) and (b) in Figs. 3 and 4). Due to the interaction with waveguide walls, the dispersion behavior in case (b) is quite different from that in case (a) (notice two resonance frequencies and narrow bandwidth in case (b)).

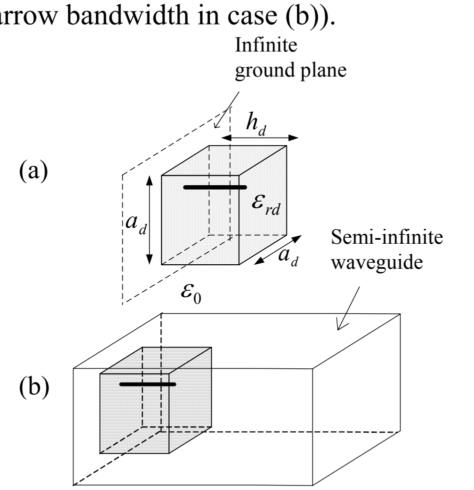

Fig. 2. (a) Geometry of infinite conductor-backed, probe-fed DRA. (b) Geometry of probe-fed DRA inside semi-infinite waveguide.

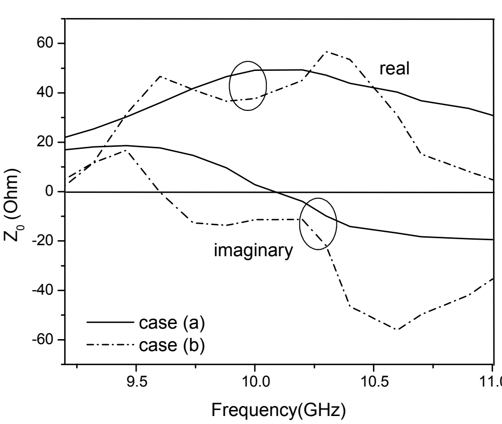

Fig. 3. Input impedance for the geometry in Fig. 2 (a), (b).

Based on the parameters from Fig. 2(b), the geometry of a waveguide-based coaxial probe-fed DRA shown in Fig. 1 was analyzed with a custom FDTD technique discussed in Section 2. For the rectangular coax of radius 1.2 mm and filled with the dielectric of permittivity ε_r = 2.56, the characteristic impedance Z_0 is 51.98 Ω, and only the TEM mode is supported as the cutoff frequency of the TE_{11} coaxial line mode is approximately 110 GHz. The probe length l_d is 4 mm and the probe axis is offset by δ_d = 1.5 mm from the waveguide centerline in the vertical direction. Fig. 5 shows the dispersion behavior of the S-parameters for this case. A -10 dB bandwidth of 10% is achieved (compared to the 3% bandwidth of a microstrip patch antenna used in a similar configuration [5]). The results in Fig. 5 are verified with commercial FDTD software [8] and exhibit very good agreement.

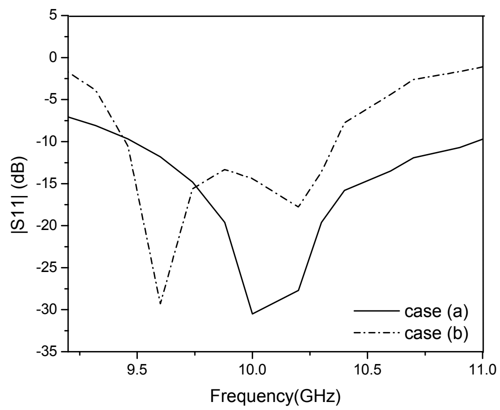

Fig. 4. Reflection coefficient for the geometry in Fig. 2 (a), (b).

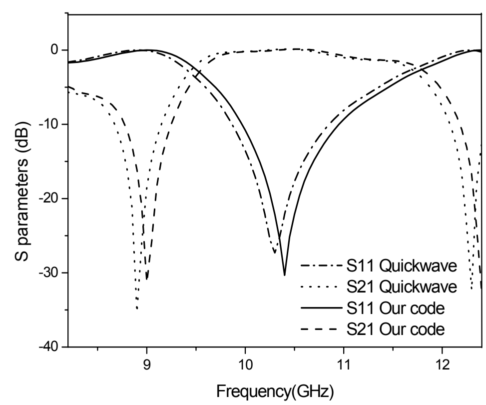

Fig. 5. S-parameters for the waveguide-based probe-fed DRA (δ_d = 1.5mm, l_d = 4mm).

For the structure operating in the X-band, the length and position of the probe in the waveguide may be used as parameters to control the matching as well as the overall frequency response. The length of the excitation probe l_d also affects significantly the overall return loss of the structure. Fig. 6 shows the return loss of the structure with different values of l_d. One can notice that a short probe couples weakly to the coaxial line. As the probe length increases, the coupling is increased and a shift of the resonant frequency is observed. As the probe becomes longer than 4.5 mm, the coupling to the coaxial line starts decreasing.

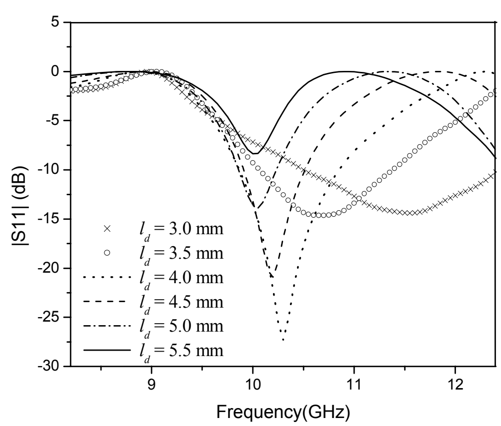

Fig. 6. Effect of varying the probe length l_d in the DRA on the return loss (δ_d = 1.5mm).

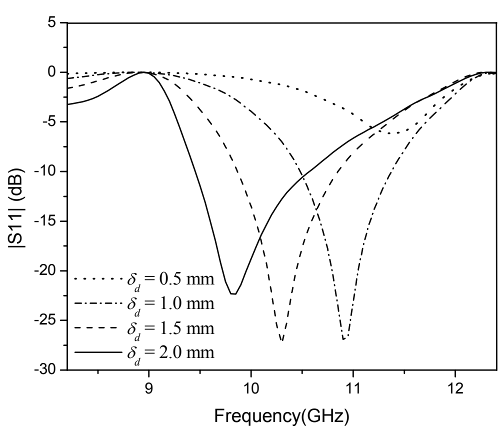

Fig. 7. Effect of varying the probe position δ_d with respect to the DRA centerline on the return loss (l_d = 4mm).

The effect of the probe position δ_d with respect to the waveguide centerline is illustrated in Fig. 7, which shows the reflection coefficient of the structure for different values of δ_d. It is clear that both the probe length and position can be used to tune and control the response in order to obtain a desired return loss over the band of interest.

4. Conclusions

A coaxial probe-fed DRA in a rectangular waveguide excited by the incident dominant mode was analyzed by using a custom FDTD method. This analysis provided the necessary information for the optimization of design parameters such as DRA dimensions and the position and length of the excitation probe. Consequently, 10% bandwidth was achieved over the frequency band of interest. This study is a useful step in the extension to the case of the DRA array for increasing the output power and the power combining efficiency of waveguide-based spatial power combiners.

5. Acknowledgment

This work was partially supported by the National Science Foundation under Grant No. ECS-0220218.

References

[1] G. P. Junker, A. A. Kishk, and A. W. Glisson, "Input impedance of dielectric resonator antennas excited by a coaxial probe," *IEEE Trans. Antennas Propagat.*, vol. 42, pp. 960-966, July 1994.

[2] G. P. Junker, A. A. Kishk, and A. W. Glisson, "Input impedance of aperture coupled dielectric resonator antennas," *IEEE Trans. Antennas Propagat.*, vol. AP-44, pp. 600-607, May 1996.

[3] A. Petosa, A. Ittipiboon, Y. M. M. Antar, D. Roscoe, and M. Cuhaci, "Recent advances in dielectric-resonator antenna technology," *IEEE Antennas and Propagation Magazine*, vol. 40, No. 3, pp. 35-47, June 1998.

[4] K. S. Kunz, and R. J. Luebbers, "The Finite Difference Time Domain Method for Electromagnetics", *CRC Press*, 1993.

[5] M. Ozkar, *Electromagnetic modeling for the optimized design of spatial power amplifiers with hard horn feeds*, Ph.D. Dissertation, North Carolina State University, 2001.

[6] K. M. Luk, and K. W. Leung, *Dielectric Resonator Antennas*, Hertfordshire, England: Research Studies Press Ltd., 2002.

[7] B. M. Kolundzija, J. S. Ognjanovic, and T. K. Sarkar, *WIPL-D*: *Electromagnetic Modeling of Composite Metallic and Dielectric Structures, Software and User's Manual.* Reading, MA: Artech House, 2000.

[8] QuickWave3D: A general purpose electromagnetic simulator based on conformal finite-difference time-domain method, v. 2.2, QWED Sp. Zo.o, Dec. 1998.

射 频 和 天 线 设 计 培 训 课 程 推 荐

易迪拓培训(www.edatop.com)由数名来自于研发第一线的资深工程师发起成立，致力并专注于微波、射频、天线设计研发人才的培养；我们于 2006 年整合合并微波 EDA 网(www.mweda.com)，现已发展成为国内最大的微波射频和天线设计人才培养基地，成功推出多套微波射频以及天线设计经典培训课程和 ADS、HFSS 等专业软件使用培训课程，广受客户好评；并先后与人民邮电出版社、电子工业出版社合作出版了多本专业图书，帮助数万名工程师提升了专业技术能力。客户遍布中兴通讯、研通高频、埃威航电、国人通信等多家国内知名公司，以及台湾工业技术研究院、永业科技、全一电子等多家台湾地区企业。

易迪拓培训课程列表：http://www.edatop.com/peixun/rfe/129.html

射频工程师养成培训课程套装

该套装精选了射频专业基础培训课程、射频仿真设计培训课程和射频电路测量培训课程三个类别共 30 门视频培训课程和 3 本图书教材；旨在引领学员全面学习一个射频工程师需要熟悉、理解和掌握的专业知识和研发设计能力。通过套装的学习，能够让学员完全达到和胜任一个合格的射频工程师的要求…

课程网址：http://www.edatop.com/peixun/rfe/110.html

ADS 学习培训课程套装

该套装是迄今国内最全面、最权威的 ADS 培训教程，共包含 10 门 ADS 学习培训课程。课程是由具有多年 ADS 使用经验的微波射频与通信系统设计领域资深专家讲解，并多结合设计实例，由浅入深、详细而又全面地讲解了 ADS 在微波射频电路设计、通信系统设计和电磁仿真设计方面的内容。能让您在最短的时间内学会使用 ADS，迅速提升个人技术能力，把 ADS 真正应用到实际研发工作中去，成为 ADS 设计专家...

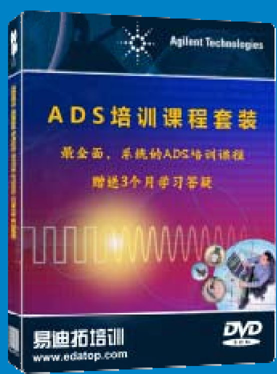

课程网址： http://www.edatop.com/peixun/ads/13.html

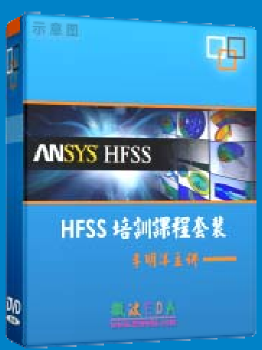

HFSS 学习培训课程套装

该套课程套装包含了本站全部 HFSS 培训课程，是迄今国内最全面、最专业的 HFSS 培训教程套装，可以帮助您从零开始，全面深入学习 HFSS 的各项功能和在多个方面的工程应用。购买套装，更可超值赠送 3 个月免费学习答疑，随时解答您学习过程中遇到的棘手问题，让您的 HFSS 学习更加轻松顺畅…

课程网址：http://www.edatop.com/peixun/hfss/11.html

CST 学习培训课程套装

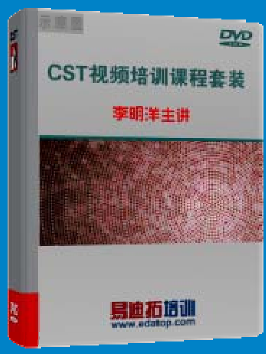

该培训套装由易迪拓培训联合微波 EDA 网共同推出，是最全面、系统、专业的 CST 微波工作室培训课程套装，所有课程都由经验丰富的专家授课，视频教学，可以帮助您从零开始，全面系统地学习 CST 微波工作的各项功能及其在微波射频、天线设计等领域的设计应用。且购买该套装，还可超值赠送 3 个月免费学习答疑…

课程网址：http://www.edatop.com/peixun/cst/24.html

HFSS 天线设计培训课程套装

套装包含 6 门视频课程和 1 本图书，课程从基础讲起，内容由浅入深，理论介绍和实际操作讲解相结合，全面系统的讲解了 HFSS 天线设计的全过程。是国内最全面、最专业的 HFSS 天线设计课程，可以帮助您快速学习掌握如何使用 HFSS 设计天线，让天线设计不再难…

课程网址：http://www.edatop.com/peixun/hfss/122.html

13.56MHz NFC/RFID 线圈天线设计培训课程套装

套装包含 4 门视频培训课程，培训将 13.56MHz 线圈天线设计原理和仿真设计实践相结合，全面系统地讲解了 13.56MHz 线圈天线的工作原理、设计方法、设计考量以及使用 HFSS 和 CST 仿真分析线圈天线的具体操作，同时还介绍了 13.56MHz 线圈天线匹配电路的设计和调试。通过该套课程的学习，可以帮助您快速学习掌握 13.56MHz 线圈天线及其匹配电路的原理、设计和调试…

详情浏览：http://www.edatop.com/peixun/antenna/116.html

我们的课程优势：

※ 成立于 2004 年，10 多年丰富的行业经验，

※ 一直致力并专注于微波射频和天线设计工程师的培养，更了解该行业对人才的要求

※ 经验丰富的一线资深工程师讲授，结合实际工程案例，直观、实用、易学

联系我们：

※ 易迪拓培训官网：http://www.edatop.com

※ 微波 EDA 网：http://www.mweda.com

※ 官方淘宝店：http://shop36920890.taobao.com